Fusion Engineering and Design 18 (1991) 407–418
North-Holland

The prediction capability for tritium production and other reaction rates in various systems configurations for a series of the USDOE/JAERI collaborative fusion blanket experiments

M.Z. Youssef, A. Kumar and M.A. Abdou

School of Engineering and Applied Science, University of California at Los Angeles, Los Angeles, CA 90024, USA

Seventeen integral fusion experiments have been perfomed so far within the USDOE/JAERI Collaborative Program on Fusion Neutronics. The main objective of these experiments is to verify the state-of-the-art neutron transport codes and nuclear data in predicting tritium production rates, in-system neutron spectra, activation reaction rates, nuclear heating, and γ decay heating in a Li_2O test assembly. In performing these experiments, the incident neutron source condition and the experimental geometrical arrangements for the test assembly were altered to study the impact of system changes on the prediction capability for the key neutronics parameters, particularly tritium production rate both locally and globally within predesignated zones in the breeding material. The test assembly itself was changed from a simple, one-material zone to a more prototypical blanket that included a stainless-steel first wall, neutron multiplier (beryllium) and coolant channels. The experiments proceeded through phase I and IIIA. In the latter phase, a line source was simulated by cyclic movement of the annular test assembly relative to the stationary point source that is located axially at the center of the inner cavity. In the latter phase, a better simulation bas been achieved to the secondary energy, and angular distributions of the incident neutron source found in Tokamak plasmas. In this paper, the results obtained by the USA, quantified in terms of the calculated-to-experimental values (C/E's) for the key neutronics parameters, are discussed for all the experiments performed so far. The change in the trends of these C/E values as one moves from one phase to another is considered by statistically treating these C/E values to arrive at a mean value for the prediction uncertainty in each experiment and an average mean value to all the experiments. This was carried out for tritium production rate, in-system spectra, and other reaction rates.

1. Introduction

The success in constructing future fusion reactors heavily depends on the accuracy involved in estimating the performance parameters of many reactor plasma physics and technology components [1,2]. One of the prime goals for utilizing fusion energy is to attain self-sufficiency in tritium in reactors based on D–T fuel cycle. Fulfilling this goal depends on how well we predict the performance parameters of the reactor components that are currently subject to large uncertainties which in turn leads to large variation in the required tritium breeding ratio (TBR). The achievable TBR, on the other hand, in various blanket concepts is limited and also subject to large uncertainties. Tritium self-sufficiency calls for adequate achievable TBR that should at least be equal to the required TBR. The uncertainties in estimating the achievable TBR depends, among other factors, on the degree of accuracy in geometrically modelling the reactor systems and blanket, the approximations introduced in the computational methods applied, and the current uncertainties in basic nuclear data.

A central approach to resolve this important design issue is to perform integral experiments to quantify the uncertainties involved in tritium production rate (TPR) in a prototypical blanket. One can, therefore, judge the adequacy of the current nuclear data and calculational tools by making comparison between the analytical predictions and calculations to key design parameters such as the TPR, in-system spectrum, reaction rates, nuclear heating and radioactivity build-up. This approach has been undertaken in the ongoing USDOE/JAERI Collaborative Program on Fusion Neutronics where several fusion-oriented integral experiments have been performed/planned utilizing the Fusion Neutronics Source (FNS) facility at the Japan Atomic Energy Research Institute (JAERI).

The objective of this paper is to give the overall uncertainties in evaluating tritium production rate, neutron spectrum, and other reaction rates inside the test assembly under varying operational and geometrical

conditions as encountered in these experiments and based on the US calculations. The counterpart of the present work that is based on JAERI's analysis is discussed in ref. [3]. Among the varying conditions considered are: a 14 MeV point source versus a simulated line source, open geometry versus closed geometry, etc. The parameter used for this purpose is the ratio of calculated-to-experimental value (C/E) for local and zonal parameters. The approach followed in the present work is to statistically calculate the effective C/E value for a given experiment (or a category of experiments) and for a particular measuring item. In this statistical treatment, both the experimental and the calculational errors involved are accounted for.

In section 2, the experiments performed so far in phase I, IIA, IIB, IIC, and IIIA are briefly described with emphasis on the difference in the geometrical arrangements among these experiments. Brief discussion on the calculational methods used is given in section 3. Section 4 is devoted to outlining the statistical treatment for C/E values obtained in each experiment. The results and discussions are given in section 5. Summary of the present work is outlined in section 6.

2. The experiments

Phase I experiments, started in October 1984 and completed in March 1986 is characterized by being performed in an open geometry with a point source. The test assembly is a cylinder of diameter $D = 60$ cm and length $L = 61$ cm constructed from Li_2O blocks of different sizes, most of them are of dimensions $5.08 \times 5.08 \times 5.08$ cm. The test assembly is loaded in the experimental cavity connecting target room ♯2 ($4.96 \times 4.96 \times 4.5$ m height), where the experiments were performed, and the large target room ♯1. The physical center of the rotating target (neutron source generator for the 14.1 MeV neutrons) is at a distance of ~ 2.48 m from the side walls and at 2.7 and 1.8 m from the ceiling and the floor level, respectively. Three categories of experiments were conducted: (1) The reference experiment (REF); the test assembly consisted of a single Li_2O material. (2) First-wall experiments; a 0.5 cm thick stainless-steel first wall (316SS) was placed in front of the Li_2O assembly, then a 0.5 cm thick polyethylene (PE) plate was placed between the first wall and the assembly. This sequence of experiments were repeated but a 1.5 cm thick first wall was deployed instead, as shown in fig. 1a. This series of experiments is designated by WFW. (3) Beryllium experiments; three configurations were assembled, namely: 5 cm thick Be,

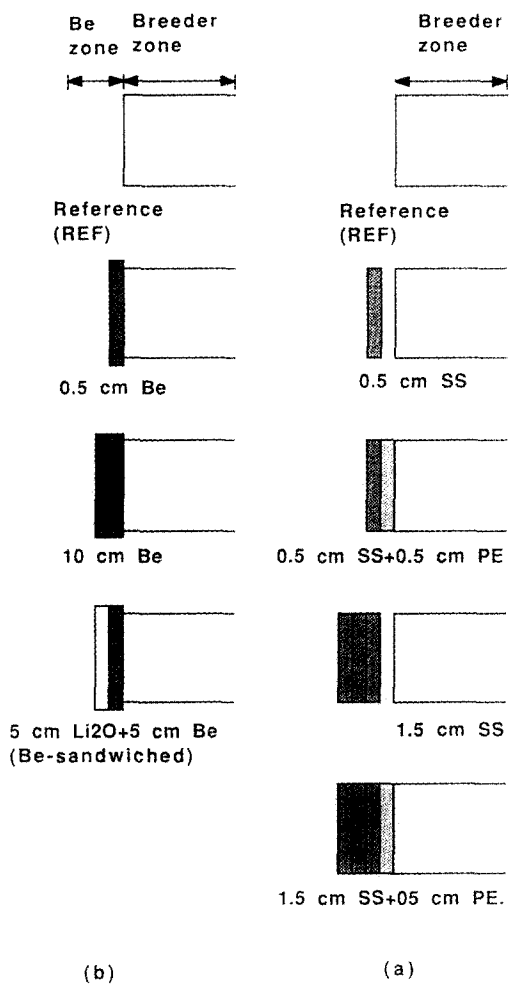

Fig. 1. Arrangements for (a) the first-wall experiments (WFW) and (b) the beryllium experiments (WBE) of Phase I.

10 cm thick Be, and 5 cm thick Li_2O + 5 cm thick Be layers were placed in front of the Li_2O assembly, separately, as shown in fig. 1b. This series of experiments is designated by WBE in the present work. Details of the measurements and analysis performed in this phase can be found in refs. [4–6].

Phase II experiments were also perfomed in target room ♯2 with a point source. In this phase, the test assembly is a rectangular shape of dimensions $86.4 \times 86.4 \times 60.71$ cm and was placed at one end of a rectangular enclosure made of Li_2CO_3 and the D–T neutron source was placed inside the cavity at a distance ~ 78 cm from the square front surface of the test assembly as shown in fig. 2. The dimensions of the inner cavity were

$87 \times 87 \times 124$ cm and the thickness of the Li_2CO_3 enclosure was 20.5 cm. A 5 cm thick PE layer was included at the outer surface of the enclosure in order to eliminate the low-energy, room-returned component of the neutrons reflected by the room walls and re-entering the test zone.

Three experiments were performed in Phase IIA. The first is the reference (REF) experiment where only the Li_2O material consituted the test assembly. In the second experiment, designated by BEF, the first five centimeters at the front were replaced by beryllium. A 5 cm thick Be layer was sandwiched between a 5 cm thick Li_2O front layer and the rest of the Li_2O test zone in the third experiment, designated BES, as shown in fig. 2a. The experiments performed in Phase IIB were similar except that the inner surface of the Li_2CO_3 enclosure was covered by a 5 cm thick Be layer in addition to a 0.5 cm thick SUS-304 first wall as shown fig. 2b. Three experiments were performed. The reference (REF) experiment had no Be layer in front of the Li_2O test zone, the beryllium front (BEF) experiment (0.5 cm thick Be layer preceded the Li_2O test assembly) without a first wall and the Be front experiment with first wall (BEFWF) of 0.5 cm thickness. Details of the measurements and analysis for Phase IIA and IIB can be found in refs. [7–15].

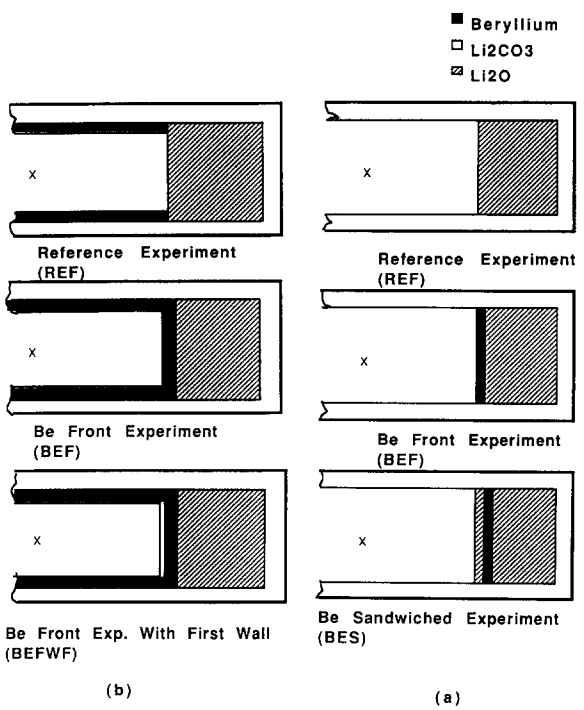

Fig. 2. Arrangements for (a) Phase IIA experiments and (b) Phase IIB experiments.

Two experiments were perfomed in phase IIC that focused on the heterogeneity effects on tritium production and other reaction rates profiles, namely: (a) the Water Coolant Channel (WCC) experiment. In this experiment simulated water coolant channels were introduced in the assembly with the dimensions shown in fig. 3a. One coolant channel was placed behind a 5 mm thick first wall that preceded the Li_2O test assembly ($\sim$ 60 cm thick) and two other channels were placed at a depth of 10 and 20 cm, respectively, and three drawers were utilized as shown in fig. 3a; and (b) the multi-layer Beryllium Edge-On experiment (BEO) in which multiple layers of Li_2O and beryllium were arranged in an edge-on, horizontally alternating configuration for a front depth of 30 cm followed by the Li_2O breeding zone and three drawers were also utilized, as shown in fig. 3b. More details on this phase can be found in refs. [16,17].

In Phase IIIA, the geometrical arrangement and source conditions were different from previous phases. An annular test assembly of length 204 cm and outer dimensions 130.1×130.1 cm with an inner square cavity of 42.55×42.55 cm was moved periodically back and forth relative to a stationary point source and hence a simulated line source was created at the central axis of the cavity. The test assembly consisted of a 1.5 cm thick 304 stainless-steel first wall followed by a 20 cm thick Li_2O zone and a 20 cm thick Li_2CO_3 zone, as shown in fig. 4. The outer surface was covered by 1.6 cm PE layer and both ends of the assembly were left open. The length of the simulated line source was 200 cm. More details on this experiment can be found in refs. [18–22]. Table 1 summarizes all the experiments considered in the present study.

Several techniques were used to measure the tritium production rate from ^6L_i (T_6). These are the Li-glass on-line method [23], the Li-metal detectors and the Li_2O pellets. Tritium production rate from $^7Li(T_7)$ were measured by the NE213 indirect method and by Li-metal and Li_2O pellet detectors. In-system spectrum was measured by small NE213 detectors [24] (in the energy range above 1 MeV) and by specially designed Proton Recoil Counter (PRC) in the energy range 1 keV–1 MeV. Many foil activation measurements were also conducted and used as spectral indices since their threshold energies ranged from 13 MeV [e.g $^{58}Ni(n, 2n)$] to as low as $\sim$ 0.5 MeV [e.g $^{115}In(n, n')^{115m}$ In].

3. Calculational methods

Both the deterministic (discrete ordinates) and the Monte Carlo methods were used in analyzing the experiments except the BEO experiment which calls for 3-D treatment by the Monte Carlo method. The MCNP code [25], version 3A, was used in analyzing phase I and IIA experiments while version 3B was applied in analyzing subsequent experiments. The pointwise continuous energy/angle cross-section library RMCCS/BMCCS, which is based on ENDF/B-V, version 2, was used in the Monte Carlo analysis. The DOT4.3 [26] and DOT5.1 codes were used in the 2-D Sn treatment. The first collision code RUFF [27] was used to generate the uncollided fluxes needed for the DOT calculations. The MATXS6 library [28] (ENDF/B-V, version 2, 80-group neutrons) was used in the DOT calculations with P5-S16 approximation while the MATXS5 (ENDF/B-V, version 2, 30-group neutrons) was applied (P3-S16) in Phase IIIA analysis [28]. The beryllium data of ENDF/B-V, LANL, and ENDF/B-VI were used in Phase IIB analysis for comparison purposes [29].

4. Statistical treatment for the C/E values

In a given experiment (or a category of experiments) and for a given reaction type r, measurements were taken at several locations. For each location i, an associated $(C/E)_{ri}$ value was obtained. In addition, an experimental error (uncertainty) and calculational error are assigned at each measuring point i, designed by σ_{rie} and σ_{ric}, respectively. The calculational error could include uncertainties due to geometrical modeling, assumptions embedded in the transport calculations used, and uncertainties associated with nuclear data. The combined uncertainty (variance) in the $(C/E)_{ri}$ value is given by

$$\sigma_{ri}^2 = \sigma_{rie}^2 + \sigma_{ric}^2, \tag{1}$$

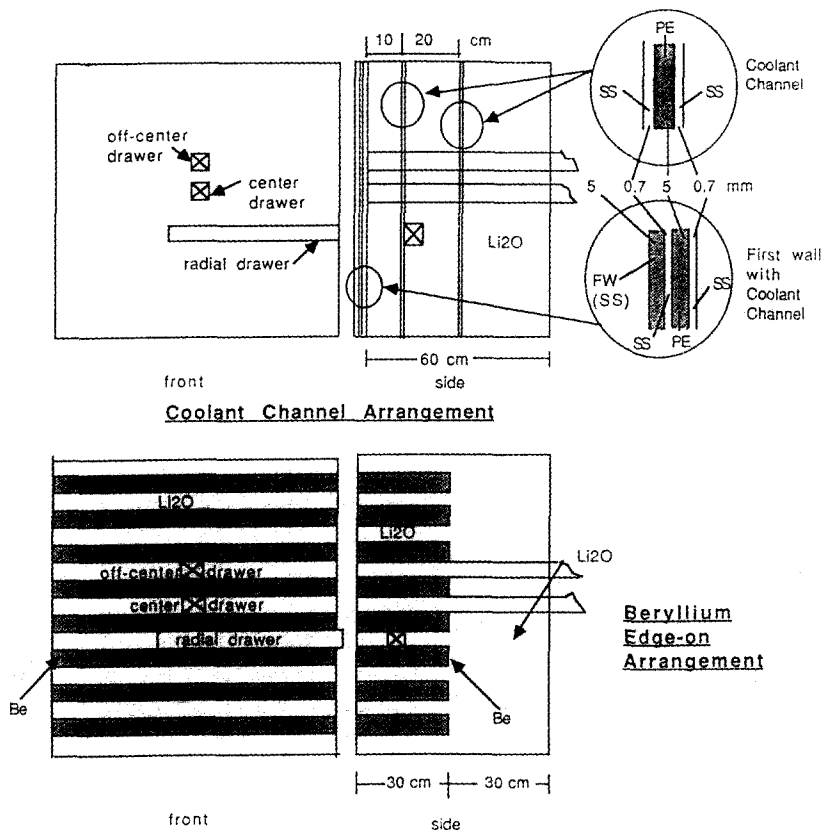

Fig. 3. The test assembly used in Phase IIC experiments: (a, top) water coolant channels (WCC) arrangement and (b, bottom) beryllium edge-on (BEO) arrangement.

assuming that the standard deviations σ_{rie} and σ_{ric} are uncorrelated. In the present analysis, the $(C/E)_{ri}$ value, designated by χ_{ri}, is weighted by a weighting factor ω_{ri}, and the mean value $\bar{\chi}_r$ for the reaction r is obtained as follows:

$$\bar{\chi}_r = \frac{\sum_{i=1}^{N} \omega_{ri}\chi_{ri}}{\sum_{i=1}^{N} \omega_{ri}} \tag{2}$$

and the standard deviation σ_r, which gives the spread around the mean value $\bar{\chi}_r$, is obtained from the expression

$$\sigma_r^2 = \frac{\sum_{i=1}^{N} \omega_{ri}^2\sigma_{ri}^2}{\left(\sum_{i=1}^{N} \omega_{ri}\right)^2} \tag{3}$$

where N is the number of the measuring locations considered. The weighting factors ω_{ri}'s are chosen to be inversely proportional to the combined uncertainty (variance) σ_{ri}^2. In this case, the $(C/E)_{ri}$ values at those

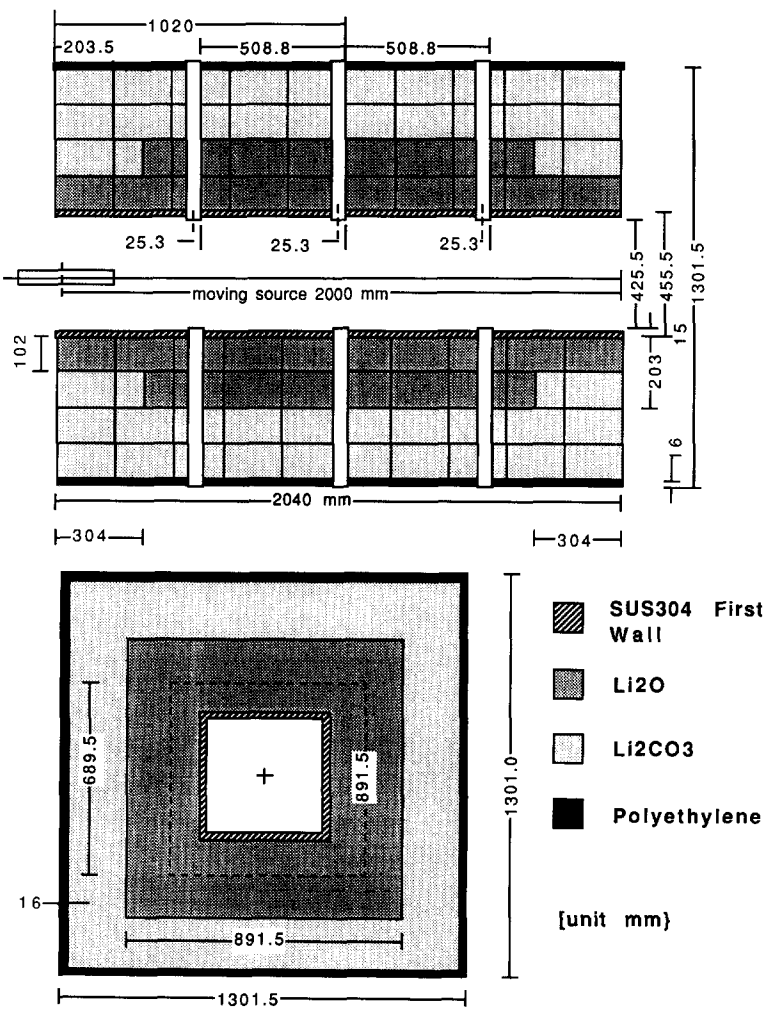

Fig. 4. Geometrical arrangement for Phase IIIA (simulated line source) experiment.

Table 1
Abbreviation for the Experiments Conducted in Phase I through Phase IIIA

Phase	Experiment (s)	Abbreviation
I	Reference exp.	REF
I	First wall exp.	WFW
I	Beryllium exp.	WBE
IIA	Reference exp.	REF
IIA	Beryllium front exp.	BEF
IIA	Beryllium-sandwiched exp.	BES
IIB	Reference exp.	REF
IIB	Beryllium front exp.	BEF
IIB	Beryllium front with first wall exp.	BEFWF
IIC	Water coolant channel exp.	WCC
IIC	Beryllium edge-on exp.	BEO
IIIA	Reference (line source) exp.	REF

measuring points whose combined uncertainties, σ_{ri}^2, are large, will have less contribution in deriving the mean value $\bar{\chi}_r$, i.e. less importance is given to the $(C/E)_{ri}$ values at these locations. Large uncertainties could be due to large experimental errors or large statistical errors in the Monte Carlo calculations, for example. Thus, if the weighting factor ω_{ri} is expressed as

$$\omega_{ri} = 1/\sigma_{ri}^2, \tag{4}$$

then, the variance σ_r^2 is obtained from the expression

$$\sigma_r^2 = 1/\sum_{i=1}^{N} (1/\sigma_{ri}^2), \tag{5}$$

where the quantities σ_{ri} appearing in eq. (4) are considered to be the absolute standard deviations at the measuring points and the mean value, $\bar{\chi}_r$, is obtained from the expression:

$$\bar{\chi}_r = \frac{\sum_{i=1}^{N} \chi_{ri}/\sigma_{ri}^2}{\sum_{i=1}^{N} 1/\sigma_{ri}^2} \tag{6}$$

5. Results and discussion

5.1. General trends for T_6 and T_7 C/E curves

Figure 5 shows the C/E values for T_6 in the reference experiment (REF) of Phase I as obtained by several codes and data (the US DOT 4.3/MATXS6 library and MCNP/RMCCS library; JAERI: DOT3.5/JACKAS library and MORSE-DD/J3PRI library; see refs. [5,6]). As seen in the US calculations, there are large discrepancies between calculations and measurements (performed by Li-glass detectors) particularly near the front surface of the test assembly. As pointed out in ref. [6], although the calculated values were corrected for self-shielding effect, the large discrepancies at front locations are due to the large uncertainty in predicting the incident low-energy component of the D–T source.

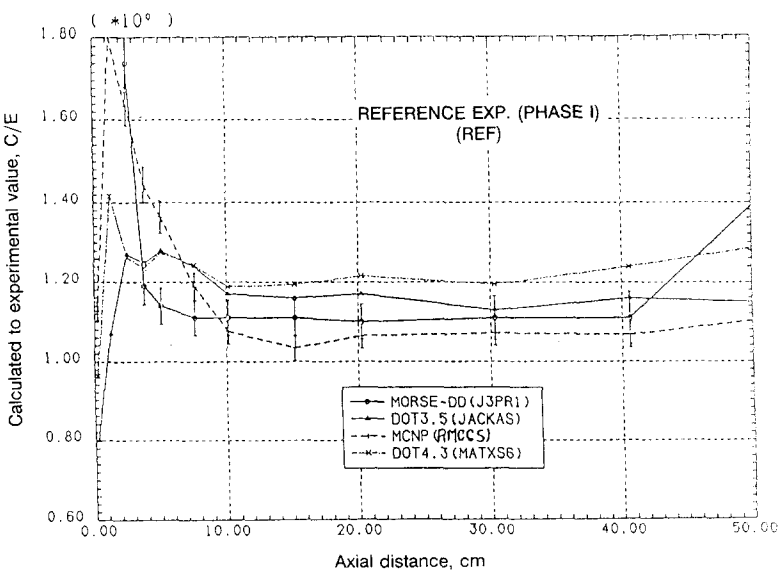

Fig. 5. The C/E values for T_6 in the reference experiment of Phase I (Li-glass measurements).

Several sources contributed to this uncertainty. Among them are: (a) difficulty in accurately modeling the complicated neutron target and room walls, (b) source separation model used in the Monte Carlo calculations [5], (c) isotropic source assumption and cylindrical modeling used in the 2-D DOT calculations, (d) sensitivity to the interpolation scheme used to extrapolate calculated values to exact measuring points near front surface (e.g. Lagrangian, log-linear) since the T_6 profiles were very steep at these locations, (e) approximations used to drive the self-shielding correction factors, and (f) uncertainties in determining the exact atomic densities of the concrete walls. The sources of uncertainties (a) to (c) are due to modeling while (d) to (e) is due to data processing approximations. Similar large uncertainties in T_6 were found in the WFW and WBE experiments of Phase I.

In general, the C/E curves for T_6 have improved in subsequent phases due to careful selection of the geometrical configuration utilized in these experiments. The T_6 profiles were found to be less steep in Phase II [9–11] and slowly decreasing in the Phase IIIA experiment [18,19,21]. It was found that the C/E values in the Be layers of Phase II are large. This was attributeed to (a) a need for large self-shielding correction factors, (b) perturbation in local neutron flux caused by the components of the Li-glass detectors, and (c) uncertainties in the secondary energy/angular distributions of neutrons emitted from the ^{9}Be(n, 2n) reactions, [29]. The C/E values for T_6 has noticeably improved in Phase IIIA (see ref. [30]).

The prediction accuracy for T_7 is better than for T_6 in Phase I. In other phases, the C/E values in bulk of the Li_2O zone are around 1.10–1.20 but larger discrepancies were found inside the 5 cm thick Be layers in Phase II.

Since our concern in this paper is to estimate the mean value for the C/E quantity inside the Li_2O zone for key parameters such as T_6, T_7, and other reaction rates, the C/E values inside other materials (e.g. beryllium, Li_2CO_3, FW, etc.) were excluded in the statistical treatment outlined in section 4. In addition, in driving the mean value $\bar{\chi}_r$ and variance σ_r^2 based on DOT results, only the experimental errors σ_{rie} were used in eq. (1). When the results of MCNP are used, the calculational errors σ_{ric} include only the statistical errors as obtained in the Monte Carlo results, i.e. no errors (uncertainties) due to modeling or nuclear data uncertainties were included in the present analysis. Estimates to uncertainties in T_6 and T_7 due to nuclear data uncertainties can be found elsewhere [31]. Furthermore, some of the experimental errors σ_{rie} were not readily available at some locations in some of the experiments

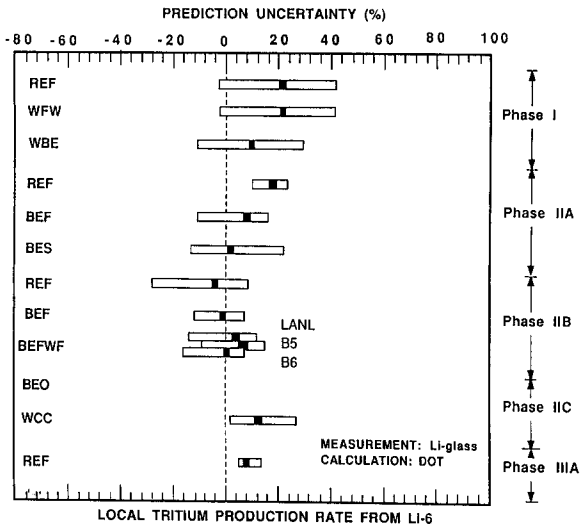

Fig. 6. The prediction uncertainty (%) for T_6, $\bar{X}_r$, based on the DOT calculations (Li-glass measurements).

at the time the present work was performed. In these cases, the following experimental errors were assumed:
- NE213 measurements ~ 6.5%
- Li-glass, Li-metal, Li_2O pellet measurements for T_6 and T_7 ~ 3.5%
- zonal TPR for T_6 and T_7 ~ 3.5%

5.2. The prediction accuracy for tritium production rate from ^{6}Li(T_6)

The prediction uncertainty (%) for a given experiment and for a given reaction rate r is quantified in terms of the parameter $\bar{X}_r = (\bar{\chi}_r - 1) \times 100$ where $\bar{\chi}_r$ is given by eq. (6) in which $\chi_{ri} = (C/E)_{ri}$. Figure 6 shows this prediction uncertainty for local T_6 in all the experiments performed so far where the measurements were performed by the Li-glass detectors and the results are those obtained by DOT calculations. These uncertainties are shown by the black bars. The middle of a black bar gives the mean value $\bar{X}_r$. The width of the bar represents the spread around this mean value and is expressed as $\bar{X}_r + \sigma_r$ and $\bar{X}_r - \sigma_r$. Shown also for each experiment is a white bar whose ends represent the maximum and the minimum values for the quantity $\bar{X}_{ri} = [(C/E)_{ri} - 1] \times 100$. Thus, a long white bar and a narrow black bar for a given experiment means that the maximum and minimum values for the quantity $\bar{X}_{ri}$ occurs at few measuring locations i while at most other locations, the quantity $\bar{X}_{ri}$ is clustered around the mean value $\bar{X}_r$. For example, in the reference (REF) experiment of Phase I, the mean value $\bar{X}_{T_6} = 21\%$ with spread

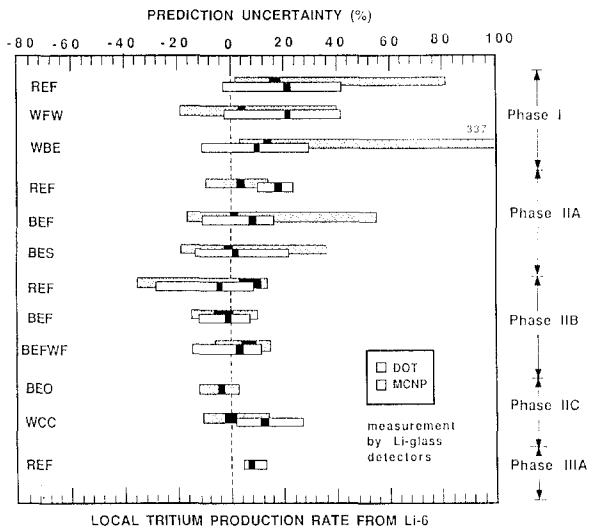

Fig. 7. The prediction uncertainty (%) for T_6, $\bar{X}_r$, based on the DOT and MCNP calculations (Li-glass measurements).

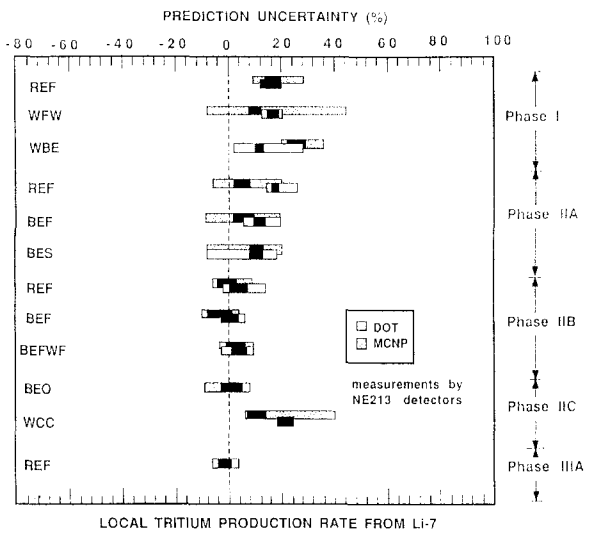

Fig. 8. The prediction uncertainty (%) for T_7, $\bar{X}_r$, based on the DOT and MCNP calculations (NE213) measurements.

$\pm\sigma_{T_6}$ of $\pm 2\%$. On the other hand, the maximum and minimum deviation from the measured value are 42% and -3% respectively. These are consistent with the values shown in Fig. 5 in DOT4.3 calculations.

By glancing at fig. 6, one can observe that the largest prediction uncertainty in T_6 was in the REF experiment of Phase I while the lowest prediction uncertainties were found in the BES experiment of Phase IIA and the BEF experiment of Phase IIB. No 2-D calculations for the BEO experiment were performed since it requires 3-D calculations. It should be noted that the prediction uncertainty in Phase IIIA experiment (simulated line source experiment) is reasonable ($\sim 8\%$) with a spread of only $\pm 1\%$. Shown also in Fig. 6 are the prediction uncertainties in the cases where ENDF/B-V (B5), ENDF/B-VI (B6) and LANL data for beryllium are used. As pointed out in ref. [29], the prediction uncertainty for T_6 with B6 data has improved while the largest uncertainty, in a relative sense, is obtained by the B5 data. This is due to the improvement in the ^{9}Be(n, 2n) corss-section itself (reduction by $\sim 10\%$ at 14 MeV) as well as the improvement in the secondary energy/angle distributions of neutrons emitted from this reaction [29].

Figure 7 shows, for comparison, the prediction uncertainties for T_6 as obtained by the MCNP calculations. The spread around the mean value expressed by σ_r is larger than those obtained by the DOT calculations, particularly in Phase IIB. In addition, large deviations in the C/E values (from unity) occur at few locations as in the WBE experiment of Phase I. However, the trend of the prediction uncertainties for T_6 is similar to DOT results. Table 2 gives the mean value $\bar{X}_r$ in each experiment as obtained by DOT and MCNP calculations. If account is made for the results of Phase I experiments, the simple average mean for the prediction uncertainty, $\bar{X}_r$ (average), in all the experiments is $\sim 8.8\%$ in DOT calculations and $\sim 4.8\%$ in MCNP calculations. These estimates are based on giving equal importance for each experiment. Excluding Phase I results, these estimates are 5.8% and 1.7%, respectively, which quantify the current uncertainties in predicting T_6 by discrete ordinates and Monte Carlo method.

Table 2
Mean values $\bar{X}_r$ for the prediction uncertainty (%) in T_6 (Measurement by Li-glass detectors).

System code	Phase I			Phase IIA			Phase IIB			Phase IIC		Phase IIIA	Average mean value	
	REF	WFW	WBE	REF	BEF	BES	REF	BEF	BEFWF	BEO	WCC	REF	w/Phase I	w/o Phase I
DOT	21	20	10	18	8	2	−4	−2	4	–	12	8	8.8%	5.8%
MCNP	18	4	14	8	2	−2	8	−4	6	−6	0	–	4.8%	1.7%

5.3. The prediction accuracy for tritium production rate from $^{7}L_i(T_7)$

The prediction uncertainty in T_7 is shown in fig. 8 where the measurements were performed by the NE213 indirect method. By examining Fig. 8, one can generally notice an overprediction in T_7, particularly in Phase I experiments, and that better prediction accuracies are observed in Phase IIB experiments, BEO experiments of Phase IIC and in Phase IIIA experiments. One can also notice that the spread around the mean values $\bar{X}_r$ are larger than those found for T_6 shown in figs. 6 and 7, and that, to a lesser extent, no spread in the white bars (DOT) and the dotted bars (MCNP), as is the case for T_6 shown in fig. 7, indicating that no extreme large deviation from unity takes place in the $(C/E)_{ri}$ values at some locations. This occurs in the C/E curves for T_6 since T_6 is sensitive to the low-energy component of the neutron flux which varies sharply between different zone boundaries.

Table 3 summarizes the mean value $\bar{X}_r$ for the prediction uncertainties in all the experiments. Also shown in this table is the average mean value as obtained by the DOT and MCNP calculations. The average mean value for the prediction uncertainties is ~ 10.4% with DOT calculations and ~ 7.5% with MCNP. These estimates are less when the results from phase I experiments are excluded [~ 8.8% (DOT) and ~ 3.8% (MCNP)]. By comparing these estimates to those obtained for T_6 (see table 2), it can be said that the prediction accuracy for T_6 is better than those for T_7. It should be emphasized that the local T_6 values are much larger than those for T_7 (by an order of magnitude) and thus the prediction uncertainties for tritium production for natural lithium is closer to those of T_6 (DOT: 6–9%, MCNP: 2–5%).

5.4 In-system spectra and other reaction rates

The prediction uncertainty in the in-system integrated spectrum above 10 MeV is shown in fig. 9 based on the NE213 measurements. As shown, the high-energy component of the neutron flux is generally underestimated in the experiments shown. The average

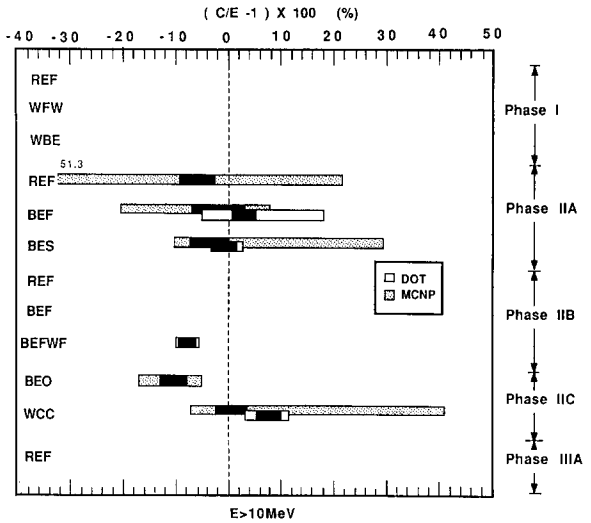

Fig. 9. The prediction uncertainty (%) for the integrated spectrum above 10 MeV.

mean value for the prediction uncertainty in this case was estimated to be −4.1% (MCNP) and 1.2% (DOT). Also, the spread around these estimates, $\pm\sigma_r$, is around ±2.5%. On the other hand, the spectrum component in the energy range 1 MeV < E < 10 MeV was found to be always overpredicted and the average mean value for its prediction uncertainties is estimated to be ~ 14% (MCNP) and ~ 31% (DOT).

The underestimation of the high-energy component of the spectrum is reflected on the C/E values for high-threshold reactions such as ^{58}Ni(n, 2n) [E_{th} ~ 13 MeV]. Figure 10 shows the uncertainty in predicting this reaction in several experiments. The average mean value for this uncertainty among the experiments considered is ~ −12% (MCNP) and ~ −13% (DOT). Since the average mean value for the underestimation in the integrated spectrum above 10 MeV is ~ −1.5% (simple average between MCNP and DOT results), thus, the cross-section for this reaction should increase by at least 10% to improve the agreement with measurements. This was pointed out in previous related analysis [16].

The average mean value for the prediction uncertainties of other reactions were also calculated. It was found

Table 3
Mean values $\bar{X}_r$ for the predication uncertainty (%) in T_7 (measured by NE213 indirect method).

System code	Phase I			Phase IIA			Phase IIB			Phase IIC		Phase IIIA	Average mean value	
	REF	WFW	WBE	REF	BEF	BES	REF	BEF	BEFWF	BEO	WCC	REF	w/Phase I	w/o Phase I
DOT	15	17	12	18	12	11	4	1	5	–	21	−2	10.4%	8.8%
MCNP	16	10	26	5	6	11	−2	−4	2	1	11	–	7.5%	3.8%

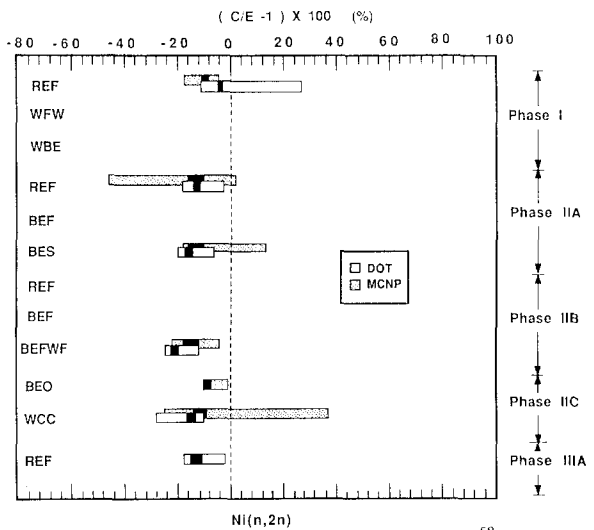

Fig. 10. The prediction uncertainty (%) for the ^{58}Ni(n, 2n) reactions.

that the prediction uncertainties for most reactions are less than $\pm 10\%$.

6. Summary

Over a dozen experiments have been performed so far within the USDOE/JAERI Collaborative Program on Fusion Neutonics to quantify the uncertainty involved in the prediction of tritium production rate, as a prime blanket characteristic in fusion blanket. In this regard, various codes and nuclear data were used in analyzing these experiments in addition to applying various measuring techniques for cross-checking experimental results. The experiments proceeded from a simple, one-material test assembly to a more protoypical assembly that included the engineering features of a fusion blanket (first wall, coolant channels, multiplier, etc.). Furthermore, the neutron source conditions were altered in these experiments to closely simulate those conditions found in Tokamak plasmas. In addition, in-system spectra and other reaction rates were measured in the test assembly and comparisons were made to the calculations.

In the present work, based on the US results, the Calculated-to-Experimental values (C/E) for tritium production rates from ^{6}Li(T_6) and ^{7}Li(T_7), as well as other reactions were treated statistically to arrive at mean statistical value $\overline{X}_r$, and the spread around it ($\pm\sigma_r$) for the prediction uncertainties in these reaction rates. An average mean value $\overline{X}_r$ (average), was also estimated, giving the same weight (importance) to each experiment. It was found that the prediction uncertainty in T_6 is $\sim 8.8\%$ and 4.8%, based on the deterministic and Monte Carlo results, respectively. When experiments in Phase I are excluded (for being less prototypical), the prediction uncertainties were reduced (5.8% (DOT), 1.7% (MCNP)). The corresponding prediction uncertainties in T_7 are 10.4% (DOT) and 7.5% (MCNP) including Phase I results and are 8.8% (DOT) and 3.8% (MCNP) when Phase I results are excluded. The prediction uncertainties for tritium production from natural lithium are close to those of T_6. It was found that the integrated spectrum above 10 MeV is underpredicted (by $\sim 1.5\%$) and overpredicted by $\sim 22\%$ (simple average of DOT and MCNP results) in the energy range 1 MeV $< E <$ 10 MeV. The prediction accuracy for other reaction rates are within $\pm 10\%$. It should be emphasized that as the present USDOE/JAERI Collaborative Program has evolved from Phase I to Phase III experiments in which the geometrical and source conditions are more prototypical of those to be found in fusion machine, the prediction uncertainties for many reactions, particularly for tritium production rates, have noticeably improved. This is in spite of the fact that the operational conditions for the simulated line source have become more complex.

Acknowledgement

The work is conduceted under the US Department of Energy, grant ♯DOE-FG03-88ER52150.

References

[1] M.Z. Youssef and M.A. Abdou, Uncertainties in prediction of tritium breeding in candidate blanket designs due to present uncertainties in nuclear data base, Fusion Technol. 9, (1986) 286–307.

[2] M.A. Abdou, E.L. Vold, C.Y. Gung, M.A. Youssef and K. Shin, D–T fuel self-sufficiency in fusion reactors, Fusion Technol. 9 (1986) 250–285.

[3] Y. Oyama, K. Kosako, M. Nakagawa and T. Nakamura, Comparative study of systems and nuclear data in C/E ratio for a series of JAERI/USDOE collaborative fusion blanket experiments, Fusion Engr. and Design, 18 (1991) 281–286, in these proceedings, Part C.

[4] T. Nakamura and M.A. Abdou, Summary of recent results from the JAERI / US fusion neutronics phase I experiment, Fusion Technol. 10 (1986) 541.

[5] M.Z. Youssef, C. Gung, M. Nakagawa, T. Mori, K. Kosako and T. Nakamura, Analysis and intercomparison for Phase I fusion integral experiments at the FNS facility, Fusion Technol, 10 (1986) 549–563.

[6] M.Z. Youssef, M.A. Abdou, C. Gung, R.J. Santoro, R.G. Alsmiller, J.M. Barnes, T.A. Gabriel, M. Nakagawa, T. Mori, K. Kosako, Y. Ikeda, and T. Nakamura, Phase I fusion integral experiments, Vol. II – Analysis, UCLA-ENG-88-15, University of California, Los Angeles, September 1988. See also JAERI-M-88-177, Japan Atomic Energy Research Institute, August 1988.

[7] M.Z. Youssef, Y. Watanabe, C.Y. Gung, M. Nakagawa, T. Mori, and K. Kosako, Analysis of neutronics parameters measured in Phase II experiments of the JAERI / US collaborative program on fusion blanket neutronics, Part II – Tritium production and in-system spectrum, Fusion Engr. and Design 9 (1989) 323–332.

[8] M. Nakagawa, T. Mori, K. Kosako, T. Nakamura, M.Z. Youssef, Y. Watanabe, C.Y. Gung, R.T. Santoro, R.G. Alsmiller, J. Barnes, and T.A. Gabriel, Analysis of neutronics parameters measured in Phase II experiments of JAERI / US collaborative program on breeder neutronics, Part I – Source characteristics and reaction rate distribution, Fusion Engr. and Design 9 (1989) 315–322.

[9] Y. Oyama, K. Tsuda, S. Yamaguchi, Y. Ikeda, C. Konno, H. Maekawa and T. Nakamura, Phase II experimental results of JAERI/USDOE collaborative program on fusion blanket neutronics experiments, Fusion Engr. and Design 9 (1989) 309–313.

[10] Y. Oyama, S. Yamaguchi, K. Tsuda, Y. Ikeda, C. Konno, H. Maekawa, T. Nakamura, K.G. Porges, E.F. Bennet and R.F. Mattas, Phase IIB experiments of JAERI/USDOE collaborative program on fusion blanket neutronics, Fusion Technol. 15, 2, Part 2B (1989) 1293–1298.

[11] M.Z. Youssef, Y. Watanabe, M.A. Abdou, M. Nakagawa, T. Mori, K. Kosako and T. Nakamura, Comparative analysis for Phase IIA and IIB experiments of the US/JAERI collaborative program on fusion breeder neutronics, Fusion Technol. 15, 2, Part 2B (1989) 1299–1308.

[12] Y. Ikeda, C. Konno, Y. Oyama, K. Oishi and T. Nakamura, Determination of neutron spectrum in D–T fusion field by foil activation technique, Fusion Technol. 15, 2 Part 2B (1989) 1287–1292.

[13] M.Z. Youssef, M.A. Abdou, Y. Watanabe and P.M. Song, The US/JAERI collaborative program on fusion neutronics; Phase IIA and IIB fusion integral experiments, the US analysis, UCLA-ENG-90-14, University of California at Los Angeles, December 1989.

[14] M. Nakagawa, T. Mori, K. Kosako, Y. Oyama and T. Nakamura, JAERI / US collaborative program on fusion blanket neutronics, analysis of Phase IIA and IIB experiments, JAERI-M-89-154, Japan Atomic Energy Research Institute, October 1989.

[15] Y. Oyama, S. Yamaguchi, K. Tsuda, Y. Ikeda, C. Konno, H. Maekawa, T. Nakamura, K. Porges, E. Bennet and R. Mattas, Phase IIA and IIB experiments of JAERI/USDOE collaborative program of fusion blanket neutronics – neutronics measurements on beryllium configuration in a full-coverage blanket geometry, JAERI-M-89-215, Part I&II, Japan Atomic Energy Research Institute, December 1989.

[16] M.Z. Youssef, A. Kumar, M. Abdou, M. Nakagawa, K. Kosako, Y. Oyama and T. Nakamura, Analysis for heterogeneous blankets and comparison to measurements: Phase IIC experiments of the JAERI/USDOE collaborative program on fusion neutronics, Fusion Technol. 19, 3, (1991) 1891–1899.

[17] Y. Oyama, S. Yamaguchi, K. Tsuda, C. Konno, Y. Ikeda, H. Maekawa, T. Nakamura, K. Porges and E. Bennet, Measured characteristics of Be multi-layered and coolant channel blankets: Phase IIC experiments of the JAERI/USDOE collaborative program on fusion neutronics, Fusion Technol. 19, 3 (1991).

[18] T. Nakmura, Y. Oyama, Y. Ikeda, C. Konno, H. Maekawa, K. Kosako, M. Youssef and M. Abdou, A line D–T neutron source facility for annular blanket experiment: Phase III of the JAERI/USDOE collaborative program on fusion neutronics, ibid (1991) 1873–1878.

[19] Y. Oyama, C. Konno, Y. Ikeda, H. Maekawa, K. Kosako, T. Nakamura, A. Kumar, M. Youssef, M. Abdou and E. Bennet, Annular blanket experiment using a line D–T neutron source: Phase IIIA of the JAERI/USDOE collaborative program on fusion neutronics, ibid (1991) 1879–1884.

[20] M.Z. Youssef, Y. Watanabe, A. Kumar, Y. Oyama and K. Kosako, Analysis for the Simulation of a line source by a 14 MeV moving point source and impact on blanket characteristics: The USDOE/JAERI collaborative program on fusion neutronics, ibid (1991) 1843–1852.

[21] C. Konno, Y. Oyama, Y. Ikeda, K. Kosako, H. Maekawa, T. Nakamura, a. Kumar, M. Youssef and M. Abdou, Measurements of the source term for annular blanket experiment with a line source: Phase IIIA of the JAERI/USDOE collaborative program on fusion neutronics, ibid (1991) 1885–1890.

[22] Y. Oyama, C. Konno, Y. Ikeda, H. Maekawa, K. Kosako, T. Nakamura, A. Kumar, M. Youssef and M. Abdou, Phase III experimental results of JAERI/USDOE collaborative program on fusion neutronics, Fusion Engr. and Design 18 (1991) 203–208, in these proceedings, Part C.

[23] S. Yamaguchi et al, An on-line method for tritium production measurement with a pair of lithium-glass scintillators, Nucl. Instrum. Meth. A245 (1987) 413.

[24] Y. Oyama et al., A small spherical NE213 scintillation detector for use in in-assembly fast neutron spectrum measurements, Nucl. Instrum. Meth. A256 (1987) 333.

[25] Los Alamos Monte Carlo Group, MCNP-A general Monte Carlo code for neutron and photon transport, version 3A, LA-7396, Rev. 2, Los Alamos National Laboratory, 1986.

[26] W.A. Rhoades and R.L. Childs, An updated version of the DOT 4 (version 4.3) one and two-dimensional neu-

tron/photon transport code, ORNL-5851. Oak Ridge National Laboratory, April 1982. Also, see CCC-429, Radiation Shielding Information Center (RSIC), 1982.

[27] L.P. Ku and J. Kolibal, RUFF-A ray tracing program to generate uncollided flux and first collision source moments for DOT4, A user's manual, EAD-R-16, Plasma Physics Laboratory, Princeton University, 1980.

[28] R.A. Macfarlane, TRANSX-CTR: A code for interfacing MATXS cross-section, libraries to nuclear transport codes for fusion systems analysis, LA-9863-MS, Los Alamos National Laboratory, February 1984.

[29] M.Z. Youssef and Y. Watanabe, Study on the accuracy of several beryllium evaluations and comparison of measured and calculated data on reaction rates and tritium production distribution, Fusion Technol. 19, 3 (1991) 1967–1973.

[30] M.Z. Youssef, A. Kumar, M.A. Abdou, Y. Oyama, K. Kosako and T. Nakamura, Post-analysis for the line source Phase IIIA experiments of the USDOE/JAERI collaborative program on fusion neutronics, Fusion Engr. and Design, 18 (1991) 265–274, in these proceedings, Part C.

[31] Y. Ikeda and M.Z. Youssef, Two-dimensional cross-section sensitivity and uncertainty analysis for tritium production rate in fusion-oriented integral experiments, Fusion Technol. 13 (1988) 616–643.